Journal of Power Sources 226 (2013) 289–298

Contents lists available at SciVerse ScienceDirect

Journal of Power Sources

journal homepage: www.elsevier.com/locate/jpowsour

Semi-interpenetrating polymer network proton exchange membranes with narrow and well-connected hydrophilic channels

Chunliu Fang [a,b], Xin Ni Toh [b], Qiaofeng Yao [b], David Julius [b], Liang Hong [b,*], Jim Yang Lee [a,b,**]

[a] National University of Singapore Graduate School for Integrative Science and Engineering, 28 Medical Drive, 117456 Singapore, Singapore
[b] Department of Chemical and Biomolecular Engineering, National University of Singapore, 4 Engineering Drive 4, 117576 Singapore, Singapore

HIGHLIGHTS

- Proton exchange membranes for the direct methanol fuel cells (DMFCs).
- A semi-interpenetrating polymer network (SIPN) based on poly(phenylene oxide).
- Use of cross-linker structure to modify membrane morphology and properties.
- Narrow and well-connected hydrophilic channels are useful for DMFC applications.
- Demonstration of membranes which surpassed Nafion® 117 in single cell tests.

ARTICLE INFO

Article history:
Received 27 August 2012
Received in revised form
29 October 2012
Accepted 1 November 2012
Available online 10 November 2012

Keywords:
Semi-interpenetrating polymer network
Poly(2,6-dimethyl-1,4-phenylene oxide)
Direct methanol fuel cell
Proton exchange membrane

ABSTRACT

Four series of semi-interpenetrating polymer network (SIPN) membranes are fabricated by thermally cross-linking aminated BPPO (brominated poly(2,6-dimethyl-1,4-phenylene oxide)) with different epoxide cross-linkers in the presence of sulfonated PPO (SPPO). The cross-link structure and hydrophobicity are found to impact the membrane morphology strongly — smaller and more hydrophobic cross-links form narrow and well-connected hydrophilic channels whereas bulky and less hydrophobic cross-links form wide but less-connected hydrophilic channels. The membranes of the former can support facile proton transport and suppress methanol crossover to result in higher proton conductivity and lower methanol permeability than the membranes of the latter. The membranes are also fabricated into membrane electrode assemblies (MEAs) and tested in single-stack direct methanol fuel cells (DMFCs). It is found that some of these SIPN membranes can surpass Nafion® 117 in maximum power density, demonstrating their potential as a proton exchange membrane (PEM) for the DMFCs.

1. Introduction

The main function of a proton exchange membrane (PEM) in the direct methanol fuel cell (DMFC) is to shuttle protons from the anode to the cathode and inhibit the diffusion of methanol at the same time [1]. A PEM typically comprises both hydrophilic and hydrophobic components. The former is used to support proton transport and usually contains sulfonic acid groups. The hydrophobic component, on the other hand, furnishes the mechanical strength and dimensional stability of the membrane [2]. In the presence of water, microphase separation occurs between the hydrophilic and hydrophobic components — the sulfonic acid groups associate to form sulfonic acid clusters which, upon connection, form the "hydrophilic channels" [3]. Protons are transported through the hydrophilic channels with the assistance of water, thus the connectedness of the channels determines the proton conductivity of any given membrane.

A continuous networks of hydrophilic channels is clearly favorable to proton transport [4,5]. Such a network may however allow the unhindered diffusion of methanol molecules, leading to significant methanol crossover and the degradation of DMFC performance. One solution to reduce methanol crossover is to narrow the hydrophilic channels to increase the resistance selectively for the larger methanol molecules. Hence PEMs for DMFCs should be designed to provide narrow and well-connected hydrophilic channels. Currently block/graft copolymers specifically designed to promote self-assembly are used to prepare these PEMs

* Corresponding author. Tel.: +65 6516 5029; fax: +65 6779 1936.
** Corresponding author. National University of Singapore Graduate School for Integrative Science and Engineering, 28 Medical Drive, 117456 Singapore, Singapore. Tel.: +65 6874 2899; fax: +65 6779 1936.
E-mail addresses: chehongl@nus.edu.sg (L. Hong), cheleejy@nus.edu.sg (J.Y. Lee).

0378-7753/$ – see front matter © 2012 Elsevier B.V. All rights reserved.
http://dx.doi.org/10.1016/j.jpowsour.2012.11.001

[6–10]. The synthesis of the block/graft copolymers is often complex and has not been designed for scalable production [11].

The semi-interpenetrating polymer network (SIPN) can be an alternative approach to deliver the desired PEM morphology of narrow and well-connected hydrophilic channels. SIPN is a special class of polymer composites where a linear or branched polymer penetrates extensively into a network of other polymers [12–14]. It offers ease of preparation and more tailorability of the PEM morphology compared with the graft/block copolymers. This is because the hydrophilic and hydrophobic components can be very intimately mixed (approaching molecular level) in an SIPN structure. The uniform dispersion of the hydrophilic component in a hydrophobic polymer network can greatly increase the connectivity of the hydrophilic channels [15–17]. Hydrophilic sulfonic acid clusters with relatively small size are also formed at the same time. The hydrophilic channels can then be made narrower to inhibit the methanol passage more effectively.

A specific methodology of using the SIPN structure for PEM fabrication is presented here. Specifically, PEMs with well-connected hydrophilic channels are produced by thermally cross-linking aminated BPPO (brominated poly(2,6-dimethyl-1,4-phenylene oxide)) with an epoxide cross-linker in the presence of sulfonated PPO (SPPO). The PPO polymer is selected as the base material because of its good mechanical properties and excellent hydrolytic stability [18]. In the SIPN structure fabricated as such, the epoxide cross-linked aminated BPPO is the polymer network host providing the mechanical properties of the PEM while SPPO is the penetrant and the proton source. In order to optimize the selectivity of proton transport over methanol permeation, four epoxides with different sizes and solubility parameters, namely 1,4-butanediol diglycidyl ether (BDE), resorcinol diglycidyl ether (RDE), bisphenol A diglycidyl ether (BADE) and poly(bisphenol A-co-epichlorohydrin) (PBAE), are used as cross-linkers. Microstructural characterizations and electrochemical measurements reveal significant differences in the PEM morphology and proton transport properties due to the use of different cross-linkers. Changes in the cross-linker structure capped by two epoxide groups are used to provide a better understanding of the impact of the molecular segment between the two epoxide end groups on the proton and methanol transport properties of SIPNs. This is helpful to the development of some rudimentary composition–morphology–property relationships for the PEM design.

2. Experimental section

2.1. Preparation of SIPN membranes

Sulfonated PPO (SPPO) was synthesized by a published procedure using chlorosulfonic acid as the sulfonation reagent [19]. Specifically, a calculated amount of chlorosulfonic acid (99.0–99.4%, Sigma–Aldrich) was added to a PPO (Sigma–Aldrich) solution in chloroform (99%, Merck) at room temperature over a period of 30 min under vigorous stirring. The reaction was allowed to continue for 30 more min after the addition. The precipitate from the reaction was filtered off and dissolved in NMP (*N*-methyl-2-pyrrolidone), and dried in an oven at 80 °C for solvent removal. The oven-dried solid was washed with deionized water until the rinse water was pH 6–7, and then vacuum-dried. The ion exchange capacity (IEC) of the SPPO synthesized as such was determined to be 2.07 mmol g^{-1}, or 29.8% degree of sulfonation according to the relation given in the literature [20].

The PPO-based SIPN membranes were prepared by a thermal cross-linking method. The preparation of BDE0.25 where the figure '0.25' refers to the ratio of epoxide groups to bromomethyl groups (1.0 for complete cross-linking) is given below as an example. BPPO (59.1% benzyl bromide and 40.9% aryl bromide as analyzed by ^{1}H NMR (Nuclear Magnetic Resonance) spectrometry, Tianwei Membrane Corporation Ltd. of Shandong) and SPPO were dissolved separately in NMP to a concentration of 30 mg mL^{-1} each. Excess ammonia (32%, Merck) was added to the solutions to neutralize SPPO and to aminate BPPO, respectively. A measured amount of BDE (Sigma–Aldrich) cross-linker was also added to the BPPO solution. After stirring for 1 h, the two solutions were mixed. The mixture was cast onto a glass petri dish, cured at 80 °C for 48 h and then at 100 °C for 2 h in vacuum. The membrane formed as such was acidified in 1.0 M HCl for 24 h, washed several times with distilled water and then air-dried. A polymer blend membrane was also prepared from neutralized SPPO and aminated BPPO without any cross-linker, and used as the control. All the membranes examined in this study were prepared with a $-SO_3H/-CH_2Br$ molar ratio of 5/1, which was found by screening experiments to represent a good balance between various membrane properties such as dimensional swelling and proton conductivity.

2.2. Characterizations

Transmission electron microscopy (TEM) was performed on a JEOL JEM-2010 TEM operating at 200 kV accelerating voltage. Membranes for TEM examination were first treated with a saturated solution of $Pb(NO_3)_2$ for 24 h to enhance the image contrast between ionic and non-ionic clusters. They were then rinsed with distilled water and dried under vacuum. The TEM samples were prepared by epoxy embedding (Sigma–Aldrich) and sectioned to 50 nm thin slices by an ultramicrotome (Leica). The slices were then placed on 100 mesh copper grids for TEM analysis. Scanning transmission electron microscopy (STEM) and elemental mapping by energy dispersive X-ray (EDX) spectroscopy were performed on a JEOL 2101F TEM. X-ray photoelectron spectroscopy (XPS) were collected by a Kratos Axis Ultra DLD spectrometer. All binding energies were referenced to the C1s carbon peak at 284.6 eV. The thermal properties of the membranes were evaluated by differential scanning calorimetry (DSC) on a Mettler-Toledo DSC 822e in N_2 atmosphere. Typically the membrane samples were heated from 25 to 270 °C at the rate of 10 °C min^{-1}. A Bruker DRX-400 MHz NMR spectrometer operating at 500 MHz was used for ^{13}C NMR measurements. The tensile strengths and strains of the membranes were measured by an Instron 5544 universal tester at room temperature. For the measurements, a membrane was cut into a (3 × 1 cm) rectangle which was held in flat-faced grips and pulled apart at the crosshead speed of 1 mm min^{-1}.

Water uptake (WU) by the membranes was measured by the difference in weights between the dry (W_{dry}, g) and water-saturated states (W_{wet}, g) of a membrane. Water uptake was calculated as the wt.% of the dry sample:

$$\mathrm{WU} = \left(\left(W_{\mathrm{wet}} - W_{\mathrm{dry}}\right)\Big/ W_{\mathrm{dry}}\right) \times 100\% \quad (1)$$

Membrane dimensional changes were estimated by equilibrating a sample strip in water at a fixed temperature for 24 h, and then measuring the changes in length:

$$\Delta l = ((l_{\mathrm{w}} - l_{\mathrm{d}})/l_{\mathrm{d}}) \times 100\% \quad (2)$$

where l_w and l_d are the lengths of the wet and dry membranes, respectively.

The membrane IEC was determined by acid–base titration. First, a membrane in its native H^+ form was equilibrated in 1.0 M NaCl for 24 h to fully exchange the protons with sodium cations. The acidity in the NaCl solution was then titrated with 0.01 M NaOH. The IEC (mmol g^{-1}) was calculated as the moles of exchangeable protons

per gram of the dry weight. Methanol permeability measurements were carried out using a two-compartment diffusion cell [21]. One of the compartments was filled with 2.0 M methanol solution, and the other with deionized water. A membrane fully hydrated with deionized water was fastened between the two compartments. The increase in methanol concentration in the water compartment with time was monitored by gas chromatography (Shimadzu GC2010 with flame ionization detector). Methanol permeability (P, $cm^2\ s^{-1}$) was calculated from the slope of the $C_B(t)$ *vs.* $t-t_0$ plot by the relation:

$$C_B(t) = (A/V_B)(P/L)C_A(t - t_0) \quad (3)$$

where C_A is the initial methanol concentration, $C_B(t)$ is the methanol concentration in the water compartment at time t, V_B is the volume of deionized water in the water compartment, L is the membrane thickness and A is the effective diffusional area.

Membrane proton conductivity was determined by the standard four-point probe technique. Impedance in the 1 MHz–50 Hz frequency range was measured by an Autolab PGSTAT 12 (Netherlands) potentiostat/galvanostat fitted with a FRA2 frequency response analyzer. Membrane resistance (R, Ω) was regressed from impedance measurements according to an established procedure [22]. Proton conductivity (σ, S cm^{-1}) was then calculated by the equation:

$$\sigma = L/RWd \quad (4)$$

where L is the distance between the potential-sensing electrodes, W and d are the width and thickness of the sample, respectively.

2.3. Fabrication of membrane electrode assembly (MEA) and DMFC tests

Membrane electrode assemblies (MEAs) were prepared by the hot pressing technique using the following electrodes supplied by Alfa Aesar: Pt:Ru alloy anode with 3.0 mg cm^{-2} total metal loading and Pt cathode with 2.0 mg cm^{-2} total metal loading. Nafion® solution was used as the binder for both electrodes and the active cell area was 5 cm^2. Membrane electrode assembly was fabricated by placing a membrane sample (or a Nafion® 117 membrane) between the two commercial electrodes and hot-pressed at 125 °C and 60 kg cm^{-2} for 3 min. The resultant MEA was then stored in a tightly sealed container. DMFC measurements were performed on a single-stack micro DMFC supplied by Fuel Cell Technologies Inc. A 2.0 M methanol aqueous solution was fed to the anode compartment at 5 $cm^3\ min^{-1}$ through a micropump. Dry oxygen was delivered to the cathode compartment at 50 $cm^3\ min^{-1}$. The DMFC performance was evaluated at 50 °C. As part of cell conditioning, all cells were rested in the open circuit condition for 30 min before any measurement was taken.

3. Results and discussion

3.1. Synthesis and characterization of SIPN structures

An SIPN structure is formed by mixing aminated BPPO, an epoxide cross-linker (BDE, RDE, BADE or PBAE) and neutralized SPPO, and keeping the mixture at 80 °C to improve the reaction kinetics. Aminated BPPO is synthesized by the reaction of BPPO with excess ammonia (Fig. 1a). The XPS (Fig. 2) and ^{13}C NMR spectroscopy (Fig. 3) confirm the successful completion of the synthesis. When ammonia is added to a BPPO solution, the bromomethyl ($-CH_2Br$) groups of BPPO are converted to aminomethyl ($-CH_2NH_2$) groups. The two peaks in the N1s XPS spectrum (Fig. 2b) with binding energies at about 399.0 eV and 401.3 eV are characteristics of primary amines and ammonium cations, respectively [23]. In Fig. 3b, the absence of a peak around 28 ppm characteristic of the aliphatic carbon in the bromomethyl group (peak 'a' in Fig. 3a) suggests the complete conversion of $-CH_2Br$ groups into $-CH_2NH_2$ groups [24]. When aminated BPPO is subsequently cross-linked by an epoxide cross-linker via the $-CH_2NH_2$ groups (Fig. 1b), hydroxyl groups are formed in the inter-chain covalent cross-links, which are confirmed by comparing the ^{13}C NMR spectrum of a cross-linked sample (e.g. the RDE1.0 membrane) with a sample without the epoxide cross-linker (Fig. 3b and c). Two new peaks emerge in the ^{13}C NMR spectrum of the cross-linked membrane RDE1.0, at 68.2 ppm (peak 'b') and 69.7 ppm (peak 'c'). Peaks 'b' and 'c' correspond well with carbon atoms next to a –OH group and a –O– group, respectively, indicating that the epoxide groups have reacted with the aminomethyl groups.

The neutralized SPPO is immobilized *in situ* by the cross-linked BPPO network during covalent cross-linking. The pre-neutralization of the sulfonic acid ($-SO_3H$) groups in SPPO by ammonia is an essential step. It averts the precipitation of a polymer salt in the reaction mixture due to ion pair formation between aminated BPPO and SPPO (protonated amine-sulfonate anion ion pair) [21]. Four series of uniform, self-standing membranes cross-linked by different epoxides are obtained after the evaporation of the NMP solvent. Post-treatment of the membranes in HCl solution re-acidified the SPPO, finalizing the preparation of the SIPN membranes. Based on the $-SO_3H/-CH_2NH_2$ ratio used for membrane preparation, the acidic $-SO_3H$ groups are present in stoichiometric excess. Some of the $-SO_3H$ groups would develop

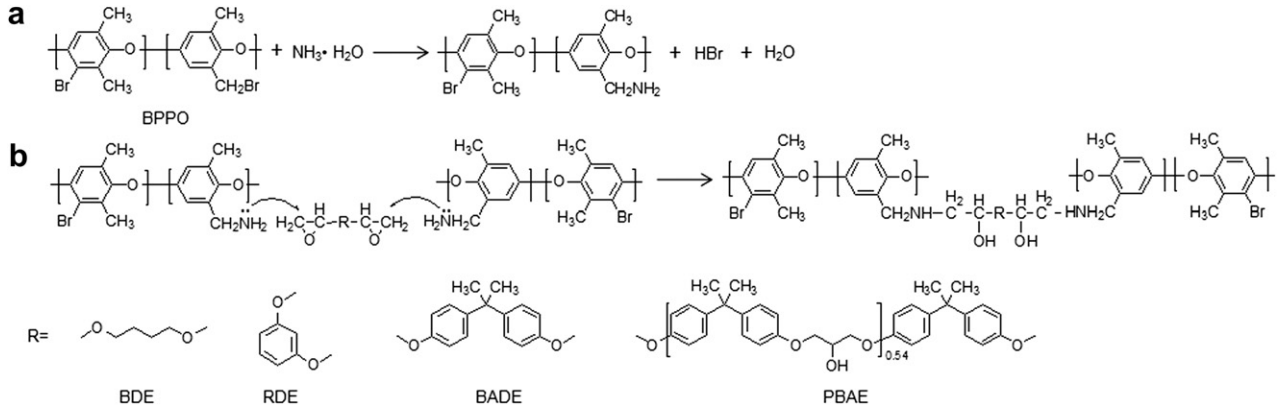

Fig. 1. Schematic of (a) synthesis of aminated BPPO and (b) covalent cross-linking between aminated BPPO and epoxide cross-linkers.

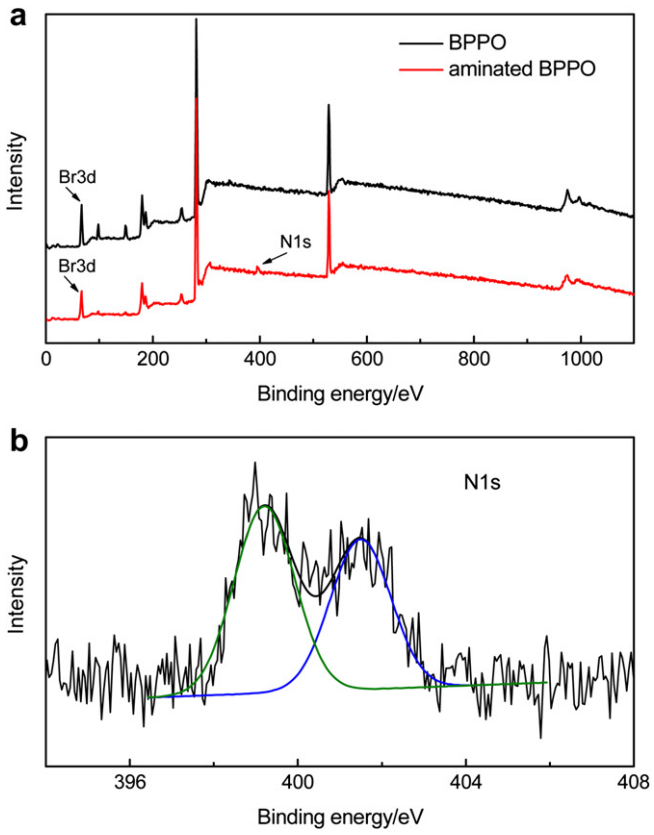

Fig. 2. (a) XPS spectra of BPPO and aminated BPPO, (b) N1s core-level spectrum of aminated BPPO, where the green and blue peaks represent the primary amines and ammonium cations, respectively. (For interpretation of the references to colour in this figure legend, the reader is referred to the web version of this article.)

ion pairs with unreacted $-CH_2NH_2$ groups or with the amine moieties formed by the covalent cross-linking reaction. The remaining $-SO_3H$ groups are free to sustain proton transport in the membrane.

3.2. Composition–morphology–property relationships

The chain structure and polarity of polymers have a strong influence on the membrane morphology [3,4,25–31]. In order to better understand the causative relationship, the effects of cross-link size and solubility parameter, and the amount of cross-linker used on membrane morphology (by TEM) are examined. The size (V, $cm^3\ mol^{-1}$) and solubility parameter (δ, $(cal\ cm^3)^{0.5}$) of the cross-links between two epoxide groups are estimated by previously published methods [32,33] and are summarized in Table 1. Both "V" and "δ" follow an increasing trend in the order of BDE < RDE < BADE < PBAE. A higher δ value indicates decreasing hydrophobicity of the cross-link.

The morphology of the SIPN membranes is examined by TEM. Four images of the 0.5 series SIPN membranes are used as comparative examples in Fig. 4. The dark spots in the TEM images are sulfonic acid clusters stained by Pb^{2+} ions to enhance the image contrast [7]. The EDX elemental mapping confirms the simultaneous presence of Pb^{2+} and sulfur in these spots (Fig. 5). Fig. 5b and c is the element maps of S and Pb for the Pb^{2+} stained RDE0.75 membrane cross-section shown in Fig. 5a. The bright spots in the EDX maps are in registration with each other, and correspond well with the dark spots in the TEM image (Fig. 5a). The superimposability of these measurements confirms that the dark spots are Pb^{2+} exchanged sulfonic acid groups.

The TEM images in Fig. 4 show a very different morphology of BDE0.5 from the other three SIPN membranes (i.e., RDE0.5, BADE0.5 and PBAE0.5): the sulfonic acid clusters are significantly

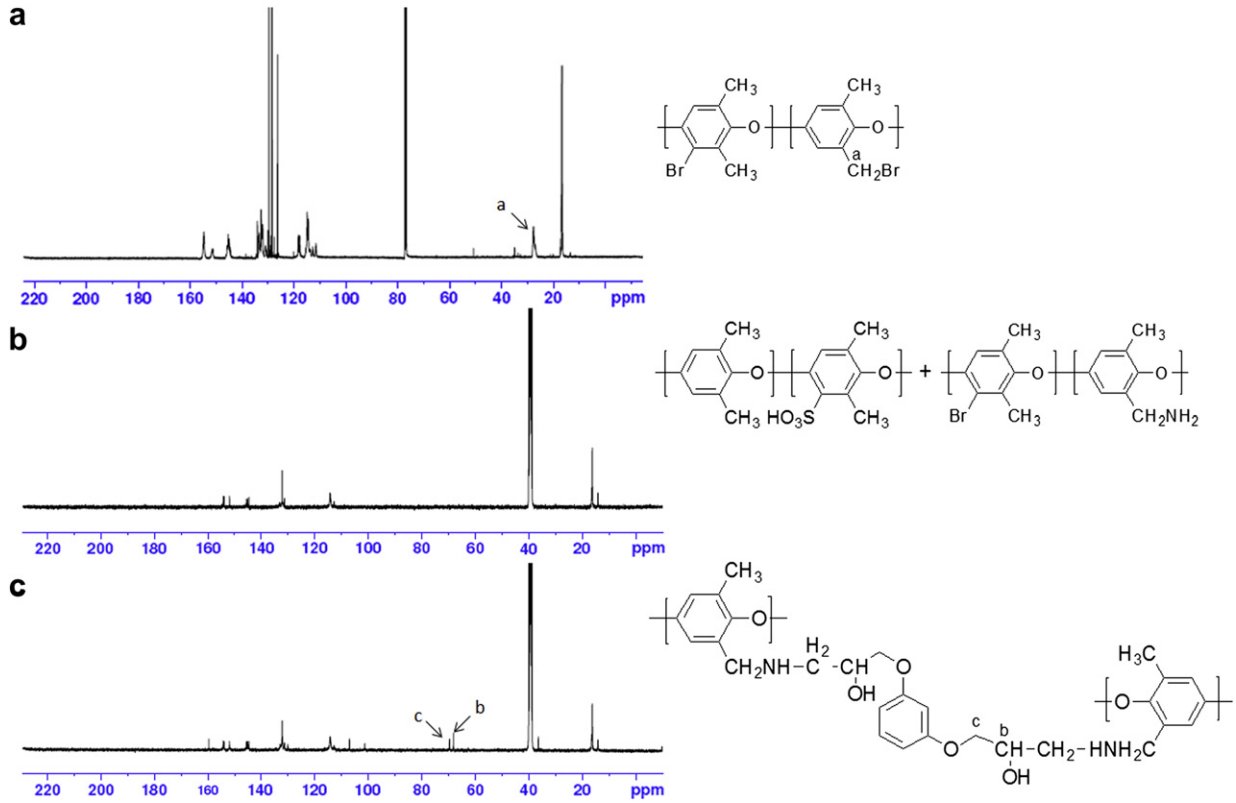

Fig. 3. ^{13}C NMR spectra of (a) BPPO, (b) blend membrane of SPPO and aminated BPPO and (c) RDE1.0 membrane.

Table 1
Calculated size and solubility parameters of cross-links between two epoxide groups.

	M (g mol^{-1})	V[a] (cm^3 mol^{-1})	ρ (g cm^{-3})	$\sum F$[b] [(cal cm^3)$^{0.5}$ cm^3 mol^{-1}]	δ[c] [(cal cm^3)$^{0.5}$]
BDE	116.3	109.2	1.01	938	8.17
RDE	136.2	114.6	1.19	1064	9.31
BADE	254.4	209.6	1.21	2057	9.80
PBAE	291.0	329.2	0.88	3432	10.38
Methanol	–			–	14.51[d]
Water	–			–	23.41[d]

[a] Data from the previous article [32].
[b] Total molar attraction constant can be estimated by simple addition of group contributions [33]. The effect of conformations was not taken into account.
[c] The solubility parameter can be calculated via $\delta = \rho \sum F/M$, where M is the molecular weight, ρ is the density.
[d] Data from handbook [49].

smaller in BDE0.5. This is taken as an indication of a smaller extent of phase separation in this particular membrane matrix. The size and solubility parameter of the BDE cross-link are smaller than the other three cross-links (RDE, BADE and PBAE). This enables the formation of a relatively dense hydrophobic membrane structure with good dimensional stability in the aqueous solution. The movement of SPPO is constrained, which limits the aggregation of sulfonic acid groups into large ionic clusters. The large number of small sulfonic acid clusters in BDE0.5 should increase the possibility of developing narrow and well-connected hydrophilic channels upon hydration [34], as shown in the illustration of Fig. 6a. On the contrary, the bulkier RDE, BADE and PBAE cross-links would space out the cross-linked polymer chains, resulting in more freedom for the SPPO polymer segmental motion. In addition, the relatively high solubility parameters of RDE, BADE and PBAE cross-links stimulate water permeation and consequently promote the aggregation of sulfonic acid groups into large clusters. The larger sulfonic acid clusters in RDE0.5, BADE0.5 and PBAE0.5 are however more isolated, and the formation of wider but less-connected hydrophilic channels is more likely to occur (Fig. 6b).

The effect of cross-linker amount on membrane morphology is investigated next. The BDE membranes will be used for discussion (Fig. 7) as their results are typical of the other three SIPN membranes (see Figs. S1–S3 in Supporting Information). All four series of the SIPN membranes display the same trend of morphology variations: increasing isolation of the sulfonic acid clusters with increasing cross-linker amount. This is because a high cross-linking degree would interrupt the continuity of the hydrophilic channels by forming dead-ends in the latter. Dead-ends are an impediment to the development of a contiguous network of hydrophilic channels. The TEM images mirror the difficulty in Pb^{2+} staining due to the diffusion limitations of dense membranes.

In order to determine the relation between membrane composition and transport properties, the IEC and proton conductivity of the membranes are measured and plot against the epoxide to $-CH_2Br$ ratio in Fig. 8. The measured IEC value of Nafion® 117 is 0.90 mmol g^{-1}. Its good agreement with the literature value is a validation of the measurement method [35]. The measured proton conductivity of Nafion® 117 of 0.05 S cm^{-1} is also included in Fig. 8b for reference. A decreasing trend of IEC and proton conductivity with increasing cross-linker amount is observed for all four series of the SIPN membranes. It is known that proton conduction depends on the accessibility of the ionic sites in aqueous solution. The increase in the number of dead-end channels with increasing cross-linking could reduce the number of accessible sulfonic acid groups and increase the tortuosity in proton transport to result in low IEC and conductivity values. Comparison of the four series of SIPN membranes indicates generally higher proton conductivities than that of the Nafion® 117 membrane. The BDE membranes, in particular, have the highest proton conductivity of the SIPN membranes.

The high proton conductivity of the BDE membranes could be explained by membrane morphology. Generally, proton transport in PEMs can occur by three mechanisms depending on the water environment. In the surface water region of the hydrophilic channels, proton transfer occurs by the surface diffusion mechanism through a series of hops between adjacent $-SO_3^-$ groups on the channel surface [36]. In the bulk water region of the hydrophilic

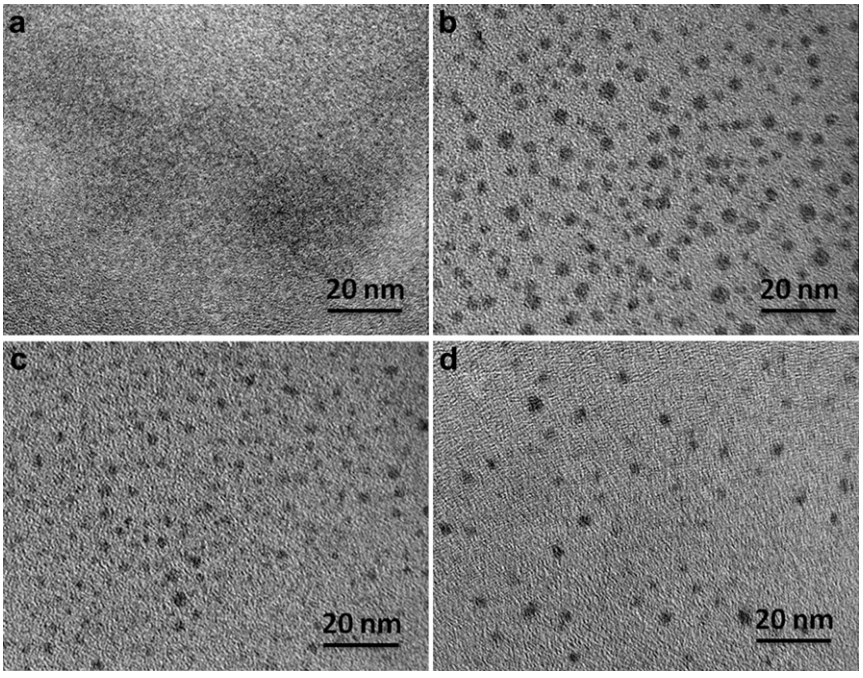

Fig. 4. TEM images of SIPN membranes: (a) BDE0.5, (b) RDE0.5, (c) BADE0.5, (d) PBAE0.5.

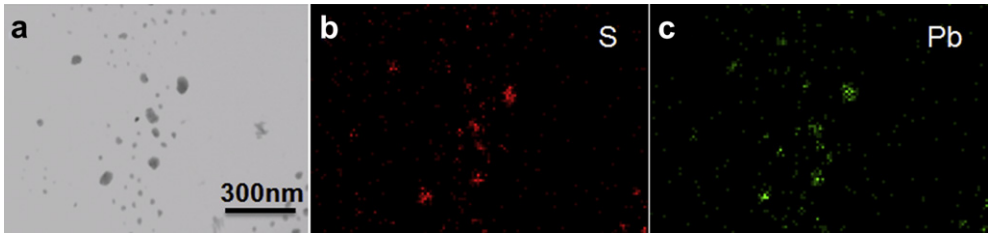

Fig. 5. EDX elemental maps of S and Pb of a Pb^{2+} stained RDE0.75 membrane. (a) TEM image of the Pb^{2+} stained RDE0.75 membrane; (b) sulfur signal; (c) lead signal (shown as bright spots).

channels, proton transfer occurs by two complementary mechanisms: the Grotthuss mechanism and the vehicular mechanism. The former involves the breaking and making of hydrogen bonds between proton-donating hydronium ions (e.g. $H_5O_2^+$ or $H_9O_4^+$) and proton-accepting water molecules; and molecular reorientation [37]. The latter occurs by the movement of proton-water aggregates, in a process similar to molecular diffusion. The overall proton conductivity is the sum of the contributions from the three mechanisms. Previous studies have indicated that the relative contributions could be differentiated by the hydration number λ (the number of water molecules per sulfonic acid group in the membrane). Specially, the dominant proton conduction mechanism at high water contents ($\lambda > 14$) is Grotthuss diffusion, while at moderately water content ($\lambda = 6$–13) the vehicular mechanism predominates [25,38]. As water content decreases ($\lambda < 6$), the strong association between SO_3^- and H_3O^+ makes it difficult for protons to transfer by the vehicular mechanism. In this case, the surface mechanism becomes increasingly important [37].

The hydration numbers λ of the SIPN membrane calculated from their IEC values and water uptake are given in Table 2. The λ values are all in the range indicative of moderate hydration, and hence the vehicular mechanism should prevail. The rate of proton diffusion by the vehicular mechanism depends on the size and the connectivity of the hydrophilic channels. Relative to the BDE membranes, the other three series of SIPN membranes should have an edge in proton conduction because their wider hydrophilic channels would allow more protons to be transported together with water molecules. The advantage is however compensated by the lower connectivity of the hydrophilic channels in RDE, BADE and PBAE membranes. The results of proton conductivity measurements suggest that the connectivity effect outweighed the size effect on proton transport in these membranes. Therefore the BDE membranes benefit from a highly connective network of hydrophilic channels where the vehicular diffusion of protons could contribute to high proton conductivity.

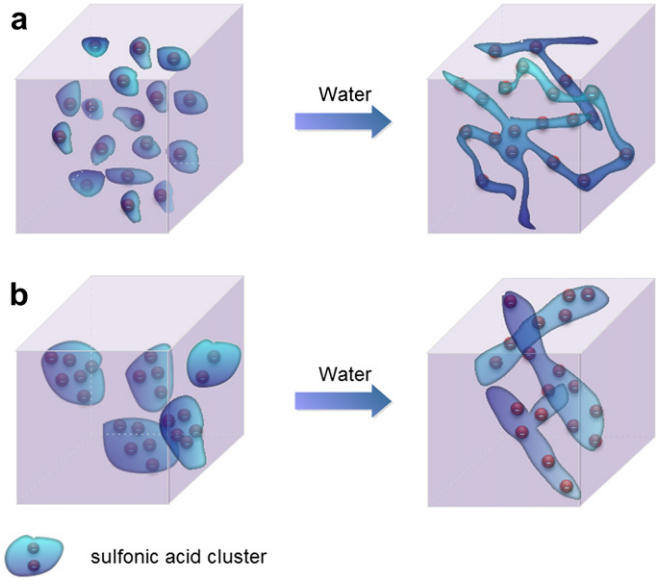

Fig. 6. Illustrations showing the sulfonic acid clusters in SIPN membranes formed with different cross-links. (a) Small and more hydrophobic cross-links form small and numerous sulfonic acid clusters, which expand into narrow but well-connected hydrophilic channels upon hydroation. (b) Bulky and less hydrophobic cross-links form large but isolated sulfonic acid clusters, thus wide hydrophilic channels with more dead-ends are formed upon hydration.

Methanol transport occurs in the same hydrophilic channels along with protons and water by a vehicular-like mechanism. Hence, methanol permeability is strongly affected by the size and the connectivity of the hydrophilic channels. The methanol permeability of the membranes varied from 3.22×10^{-7} cm^2 s^{-1} (BADE0.25) to $\sim 2.29 \times 10^{-7}$ cm^2 s^{-1} (BADE1.0) (Fig. 9), which are an order of magnitude lower than the methanol permeability of Nafion® 117 measured under the same experimental conditions (2.01×10^{-6} cm^2 s^{-1}). Hence the SPIN membranes have generally good methanol barrier properties. The methanol permeabilities of BDE, RDE and BADE membranes are about the same, and are higher than the methanol permeability of the PBAE membranes. The good connectivity of the hydrophilic channels in the BDE membranes does not however cause an increase in methanol crossover because the small channel size impedes methanol diffusion. Relative to protons, the size effect affects methanol molecules more because of the larger complexation size of the latter (i.e., self-associations as $(CH_3OH)_a$, water-bound complexes, $(CH_3OH)_m(H_2O)_n$, and proton bound complexes $H^+(CH_3OH)_b$) [39–42]. The good methanol-barrier properties of the RDE and BADE membranes, on the other hand, are more likely due to the increase in the tortuosity and dead-ends of the channels. The same reason could also explain the very low methanol permeability of the PBAE membranes formed by the extremely bulky PBAE cross-linker.

3.3. Dimensional swelling, mechanical property and oxidative stability of SIPN membranes

A high water uptake can cause excessive membrane swelling, resulting in the delamination of MEA at the membrane–electrode interface and consequently poor fuel cell durability [43]. Small membrane dimensional changes are therefore desirable for the DMFC operation. The dimensional swelling of the SIPN membranes is measured at 25 and 80 °C respectively, the two ends of the operating temperature typical for DMFCs (Fig. 10). All SIPN membranes have smaller dimensional swelling than the uncross-linked SPPO/aminated BPPO blend membranes especially at the higher temperature. This is clearly due to the effectiveness of a cross-linked network in restraining swelling. The RDE, BADE and PBAE membranes undergo comparable or smaller dimensional changes than the BDE membranes, even though water uptake in the

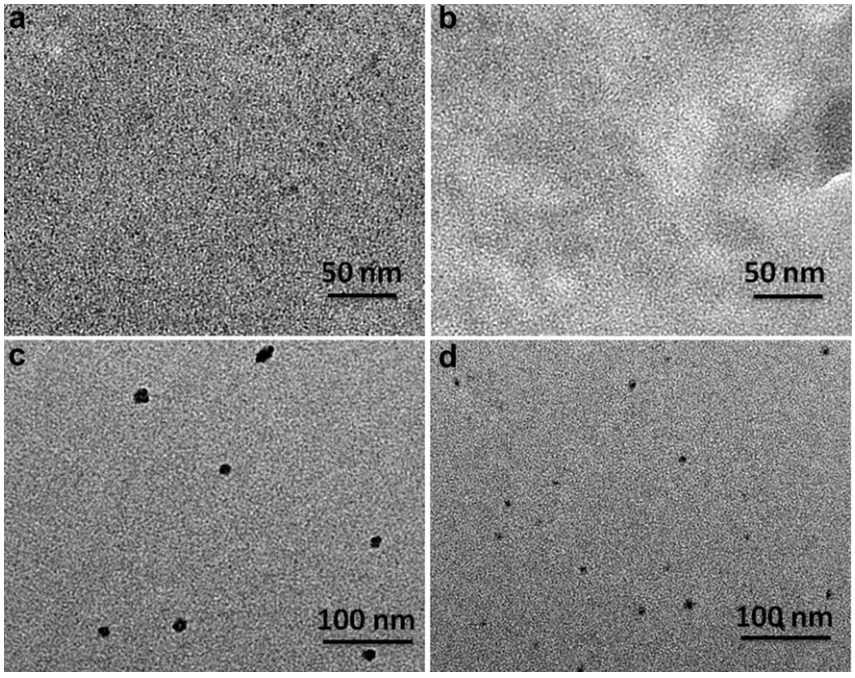

Fig. 7. TEM images of SIPN membranes: (a) BDE0.25, (b) BDE0.5, (c) BDE0.75, (d) BDE1.0.

former is higher. The discrepancy between water uptake and membrane swelling could be explained by the larger free volume of the RDE, BADE and PBAE membranes. In these membranes, the cross-links serve as spacers to keep the polymer chains at a greater distance. The spacing-out effect results in more free volume for water absorption. The bulky cross-links, however, inhibit the SPPO segmental motion, thus restraining the swelling of the SPPO polymers in water. Hence, the dimensional changes in RDE, BADE and PBAE SIPN membranes remains small.

The above effect of the cross-linkers is also reflected by DSC measurements. Two endothermic peaks at around 125 °C and 240 °C are detected in the DSC curves of the SIPN membranes (Fig. S4 in Supporting Information). Although the assignment of the first peak (I) at lower temperature remains contestable [44,45], it is more likely associated with the rotation of the phenyl rings in short PPO segments. The high-temperature peak (II) should relate more to intermolecular attractions (i.e., dipole–dipole interactions between $-SO_3H$ groups and ion pair interactions) and polymer chain movements [46]. Generally, an endothermic peak at high temperature in the DSC curve is an indication of constrained polymer chain movements, and high energy barrier in phase

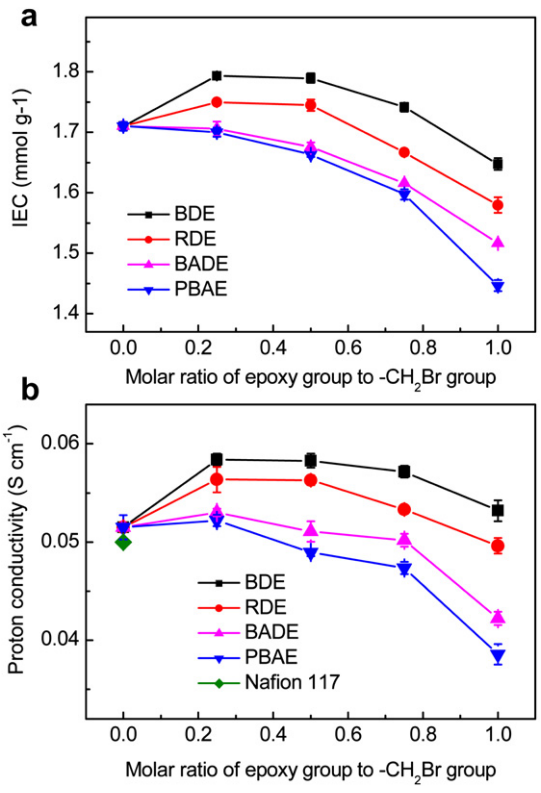

Fig. 8. IEC (a) and proton conductivity (b) of SIPN membranes.

Table 2
The water uptake (WU, %), hydration number (λ, the number of water molecules per sulfonic acid groups in membranes), and mechanical properties of SIPN membranes.

Membrane	WU (%)	λ	Tensile strength (Mpa)	Maximum elongation (%)
SPPO/aminated BPPO	24.30	7.89	18.90	13.28
BDE0.25	28.41	8.82	18.83	17.53
BDE0.5	29.71	9.22	23.57	16.99
BDE0.75	26.31	8.40	26.94	13.16
BDE1.0	20.71	6.97	31.29	11.45
RDE0.25	24.30	7.89	18.03	19.63
RDE0.5	29.94	9.50	23.93	15.59
RDE0.75	30.31	9.68	26.16	13.19
RDE1.0	26.39	8.78	30.69	11.42
BADE0.25	24.30	7.89	17.33	18.36
BADE0.5	34.38	11.24	24.36	16.13
BADE0.75	35.94	11.96	27.65	15.24
BADE1.0	31.48	10.86	30.84	12.09
PBAE0.25	24.30	7.89	20.16	16.62
PBAE0.5	34.45	11.26	25.28	13.85
PBAE0.75	32.86	10.99	27.12	13.91
PBAE1.0	30.62	10.70	37.70	13.76
Nafion® 117	20.10	12.41	17.85	177.00

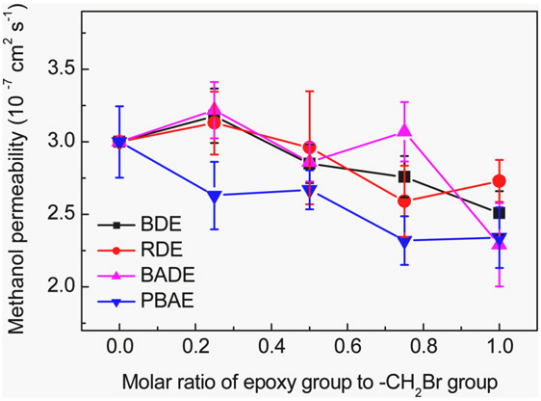

Fig. 9. Methanol permeability of SIPN membranes.

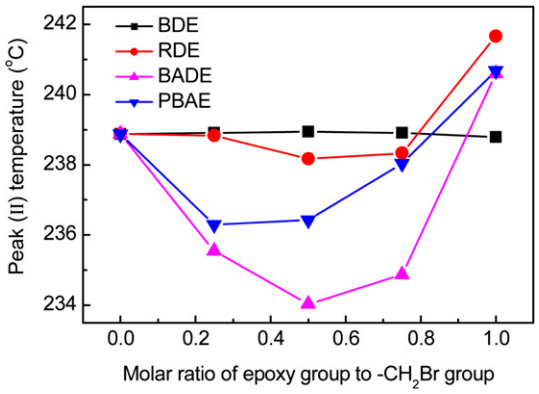

Fig. 11. The transition peak (II) temperature of SIPN membranes.

transition. Consequently the second peak (II) in Fig. 11 is carefully analyzed to provide some information on the SIPN membrane microstructure. The peak temperature is lower in the RDE, BADE and PBAE membranes than in the BDE membranes, suggesting less constrained motion of the polymer chains which is consistent with the spacing-out effect and larger free volume in membranes.

The results from the tensile strength measurements are summarized in Table 2. With the increase in the cross-linking extent, all four series of SIPN membranes show higher tensile strengths and lower strains. The measured tensile strengths and maximum elongations of the BDE, RDE and BADE SIPN membranes are in the ranges of 17.33–31.29 MPa and 11.42–19.63%, respectively. The PBAE SIPN membranes are the notable exception with much higher tensile strengths (20.16–37.70 MPa). This could be because the bulky PBAE cross-links inhibit the relative segmental motion of the polymer chains. For comparison, the tensile strength and maximum elongation of Nafion® 117 under the same test conditions are 17.85 MPa and 177.00%, respectively. Hence while the SIPN membranes are relatively rigid, they do possess sufficient mechanical strength to be used in DMFCs.

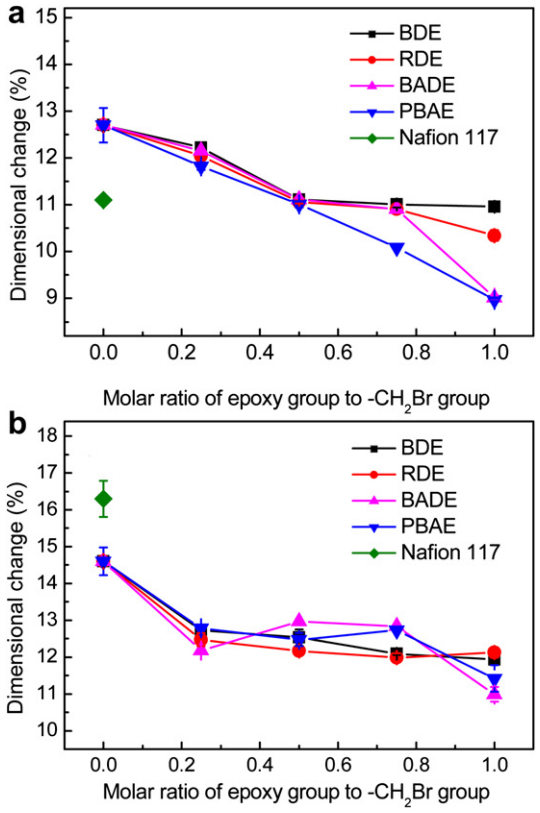

Fig. 10. Dimensional swelling in Nafion® 117 and SIPN membranes at (a) 25 °C and (b) 80 °C.

The oxidative and hydrolytic stability of the membranes are also measured and Table 3 is the summary of the measurements. The oxidative stability of the membranes is evaluated by the Fenton test (chemical stability in 3 wt.% H_2O_2 aqueous solution containing 3 ppm $FeCl_2 \cdot 4H_2O$) at 80 °C [47]. All membranes are embrittled after 1 h in the Fenton solution. Detachment of small fragments occurs to result in over 10 wt.% of weight loss. Compared to a weight loss of 23.1 wt.%–57.3 wt.% for the BADE and PBAE membranes, the BDE and RDE membranes fare better, showing more oxidative stability. This is because the oxidative attack by radical species (HO• and HOO•) should occur mostly in or in the proximity of the hydrophilic domains [48]. The high water content of BADE and PBAE membranes renders them more susceptive to the radical attack. The hydrolytic stability of the membranes is evaluated by measuring the proton conductivity before and after equilibrium in 80 °C water for two weeks. All membranes show negligible loss of conductivity.

3.4. Single-stack DMFC test

The SIPN membranes and an SPPO/aminated BPPO blend are fabricated into MEAs and tested in single-stack DMFCs. Power

Table 3
Oxidative and hydrolytic stability of SIPN membranes.

Membrane	Oxidative stability	Hydrolytic stability	
	Weight loss in Fenton's test (%)	Proton conductivity (S cm^{-1})	
		before	after
SPPO/aminated BPPO	34.4	0.051	0.046
BDE0.25	21.6	0.058	0.056
BDE0.5	19.0	0.058	0.055
BDE0.75	14.6	0.057	0.055
BDE1.0	13.3	0.053	0.050
RDE0.25	21.2	0.056	0.053
RDE0.5	20.6	0.056	0.054
RDE0.75	19.5	0.053	0.051
RDE1.0	17.3	0.049	0.047
BADE0.25	25.4	0.053	0.049
BADE0.5	23.1	0.051	0.047
BADE0.75	25.5	0.050	0.047
BADE1.0	26.1	0.042	0.038
PBAE0.25	57.3	0.052	0.048
PBAE0.5	49.0	0.049	0.045
PBAE0.75	36.2	0.047	0.043
PBAE1.0	30.3	0.038	0.034
Nafion® 117	0.5	0.050	0.048

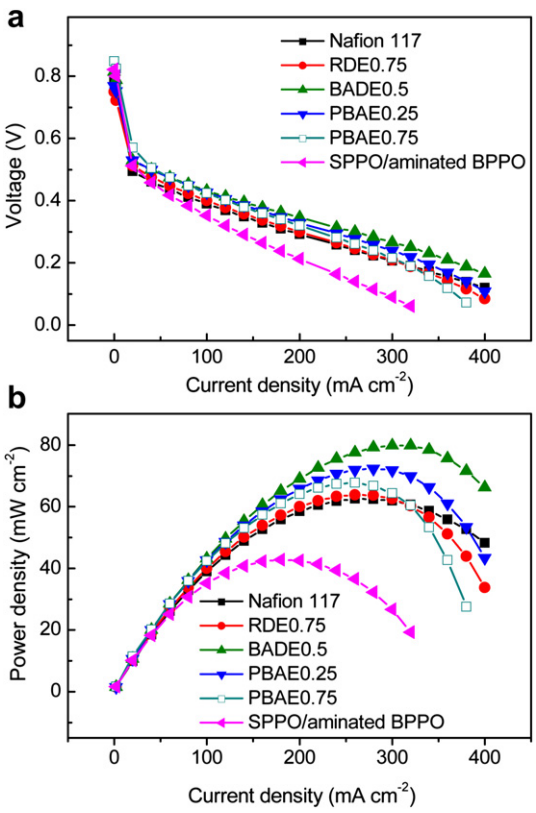

Fig. 12. Single cell performance of SIPN membranes and Nafion® 117: (a) polarization curves, (b) power density curves.

density and other fuel cell parameters are measured in order to evaluate the membrane performance under practical conditions. The RDE0.75, BADE0.5 and PBAE0.25 and PBAE0.75 membranes are able to deliver a higher maximum power density than Nafion® 117, as shown in Fig. 12. For example, the maximum power density of the BADE0.5 MEA is about 80.0 mW cm^{-2} at 310 mA cm^{-2}, about 30% higher than the Nafion® 117 MEA (62.6 mW cm^{-2} at 270 mA cm^{-2}). The open circuit voltage (OCV) is also higher with the BADE0.5 MEA (0.814 V) than with the Nafion® 117 MEA (0.793 V). Compared with the four SIPN membranes, the cell performance of the SPPO/aminated BPPO blend membrane is relatively poor with a maximum power density of only 42.9 mW cm^{-2}. The improved performance of the SIPN membranes in DMFCs could be attributed to their low methanol permeability. The polarization curves and power density plots for all of the SIPN membranes can be found in Supporting Information (Figs. S5–S8). In general the single cell performance of most RDE, BADE and PBAE membranes is better than that of the BDE membranes. While the proton conductivity of the BDE membranes is higher than the other three series of membranes, the BDE membranes do not perform as well at the MEA level. The reason remains unknown but the difference in current density between conductivity measurements (zero current density) and single cell tests (high current densities) could be a contributing factor (possible changes in polymer dynamics). This is an indication of the importance of single cell tests for the objective evaluation of PEM performance.

4. Conclusions

The SIPN membranes with narrow and well-connected hydrophilic channels have been synthesized by thermally cross-linking BDE with aminated BPPO in the presence of linear SPPO. The resulting membranes exhibit higher proton conductivity and lower methanol permeability when compare with Nafion® 117. Three other series of SIPN membranes are also prepared using different cross-linkers (i.e., RDE, BDE, and PBAE). Comparison between these four series of membranes reveals the importance of the cross-link structure on membrane morphology. Specifically, membranes formed with small and more hydrophobic cross-links (i.e., BDE) have smaller sulfonic acid clusters than membranes formed with bulky and less hydrophobic cross-links (i.e., RDE, BADE and PBAE). This difference is attributed to the dense structure and water rejection property in the former which impede the aggregation of sulfonic acid groups into larger clusters. There are however more small sulfonic acid clusters in the BDE membranes to increase the extent of channel connection upon hydration. The sulfonic acid clusters in RDE, BDE, and PBAE membranes are larger but more isolated, hence only wider but less-connected hydrophilic channels are formed after hydration. As a result of the difference in channel morphology, the BDE membranes yield higher proton conductivity than the other three series of membranes. This study provides an alternative strategy to using block/graft copolymers for the preparation of membranes with narrow and well-connected hydrophilic channels. Some general composition–morphology–property relationships are discovered which could be useful for the design of other SIPN PEMs.

Acknowledgement

C. Fang acknowledges the research scholarship support from the National University of Singapore Graduate School for Integrative Science and Engineering (NGS).

Appendix A. Supplementary material

Supplementary material related to this article can be found at http://dx.doi.org/10.1016/j.jpowsour.2012.11.001.

References

[1] V. Neburchilov, J. Martin, H.J. Wang, J.J. Zhang, J. Power Sources 169 (2007) 221–238.
[2] M.A. Hickner, B.S. Pivovar, Fuel Cells 5 (2005) 213–229.
[3] W.Y. Hsu, T.D. Gierke, J. Membr. Sci. 13 (1983) 307–326.
[4] K.D. Kreuer, J. Membr. Sci. 185 (2001) 29–39.
[5] M.A. Hickner, H. Ghassemi, Y.S. Kim, B.R. Einsla, J.E. McGrath, Chem. Rev. 104 (2004) 4587–4611.
[6] B. Bae, K. Miyatake, M. Watanabe, Macromolecules 42 (2009) 1873–1880.
[7] M. Lee, J.K. Park, H.S. Lee, O. Lane, R.B. Moore, J.E. McGrath, D.G. Baird, Polymer 50 (2009) 6129–6138.
[8] J.F. Ding, C. Chuy, S. Holdcroft, Adv. Funct. Mater. 12 (2002) 389–394.
[9] A. Roy, X. Yu, S. Dunn, J.E. McGrath, J. Membr. Sci. 327 (2009) 118–124.
[10] E.P. Jutemar, P. Jannasch, J. Membr. Sci. 351 (2010) 87–95.
[11] T. Higashihara, K. Matsumoto, M. Ueda, Polymer 50 (2009) 5341–5357.
[12] H. Pan, H. Pu, D. Wan, M. Jin, Z. Chang, J. Power Sources 195 (2010) 3077–3083.
[13] L. Chikh, V. Delhorbe, O. Fichet, J. Membr. Sci. 368 (2011) 1–17.
[14] P.P. Kundu, B.T. Kim, J.E. Ahn, H.S. Han, Y.G. Shul, J. Power Sources 171 (2007) 86–91.
[15] G. Rohman, D. Grande, F. Laupretre, S. Boileau, P. Guerin, Macromolecules 38 (2005) 7274–7285.
[16] I. Gitsov, C. Zhu, J. Am. Chem. Soc. 125 (2003) 11228–11234.
[17] X. Wu, G. He, S. Gu, Z. Hu, P. Yao, J. Membr. Sci. 295 (2007) 80–87.
[18] T.W. Xu, D. Wu, L. Wu, Prog. Polym. Sci. 33 (2008) 894–915.
[19] R.Y.M. Huang, J.J. Kim, J. Appl. Polym. Sci. 29 (1984) 4017–4027.
[20] B. Kruczek, T. Matsuura, J. Membr. Sci. 146 (1998) 263–275.
[21] R.Q. Fu, D. Julius, L. Hong, J.Y. Lee, J. Membr. Sci. 322 (2008) 331–338.
[22] Y. Sone, P. Ekdunge, D. Simonsson, J. Electrochem. Soc. 143 (1996) 1254–1259.
[23] Z.P. Cheng, X.L. Zhu, Z.L. Shi, K.G. Neoh, E.T. Kang, Surf. Rev. Lett. 13 (2006) 313–318.
[24] D.M. White, S.A. Nye, Macromolecules 23 (1990) 1318–1329.
[25] K.D. Kreuer, S.J. Paddison, E. Spohr, M. Schuster, Chem. Rev. 104 (2004) 4637–4678.
[26] K.D. Kreuer, M. Ise, A. Fuchs, J. Maier, J. Phys. IV 10 (2000) 279–281.
[27] G. Gebel, P. Aldebert, M. Pineri, Polymer 34 (1993) 333–339.

[28] G. Gebel, R.B. Moore, Macromolecules 33 (2000) 4850–4855.
[29] G. Gebel, Polymer 41 (2000) 5829–5838.
[30] T.D. Gierke, G.E. Munn, F.C. Wilson, J. Polym. Sci. Part B: Polym. Phys. 19 (1981) 1687–1704.
[31] W.Y. Hsu, T.D. Gierke, Macromolecules 15 (1982) 101–105.
[32] M.M. Coleman, C.J. Serman, D.E. Bhagwagar, P.C. Painter, Polymer 31 (1990) 1187–1203.
[33] D.A. Musale, A. Kumar, J. Appl. Polym. Sci. 77 (2000) 1782–1793.
[34] S.S. Jang, W.A. Goddard, J. Phys. Chem. C 111 (2007) 2759–2769.
[35] E.M.W. Tsang, Z.B. Zhang, A.C.C. Yang, Z.Q. Shi, T.J. Peckham, R. Narimani, B.J. Frisken, S. Holdcroft, Macromolecules 42 (2009) 9467–9480.
[36] T.J. Peckham, S. Holdcroft, Adv. Mater. 22 (2010) 4667–4690.
[37] M. Eikerling, A.A. Kornyshev, A.M. Kuznetsov, J. Ulstrup, S. Walbran, J. Phys. Chem. B 105 (2001) 3646–3662.
[38] S.J. Paddison, R. Paul, K.D. Kreuer, Phys. Chem. Chem. Phys. 4 (2002) 1151–1157.
[39] Y.A. Elabd, E. Napadensky, C.W. Walker, K.I. Winey, Macromolecules 39 (2006) 399–407.
[40] B.S. Pivovar, Y.X. Wang, E.L. Cussler, J. Membr. Sci. 154 (1999) 155–162.
[41] T.A. Zawodzinski, C. Derouin, S. Radzinski, R.J. Sherman, V.T. Smith, T.E. Springer, S. Gottesfeld, J. Electrochem. Soc. 140 (1993) 1041–1047.
[42] T.A. Zawodzinski, M. Neeman, L.O. Sillerud, S. Gottesfeld, J. Phys. Chem. 95 (1991) 6040–6044.
[43] H.P. Bi, J.L. Wang, S.W. Chen, Z.X. Hu, Z.L. Gao, L.J. Wang, K. Okamoto, J. Membr. Sci. 350 (2010) 109–116.
[44] K.A. Page, K.M. Cable, R.B. Moore, Macromolecules 38 (2005) 6472–6484.
[45] R.J. Goddard, B.P. Grady, S.L. Cooper, Macromolecules 27 (1994) 1710–1719.
[46] B.J. Liu, G.P. Robertson, D.S. Kim, M.D. Guiver, W. Hu, Z.H. Jiang, Macromolecules 40 (2007) 1934–1944.
[47] B.P. Tripathi, T. Chakrabarty, V.K. Shahi, J. Mater. Chem. 20 (2010) 8036–8044.
[48] N. Asano, M. Aoki, S. Suzuki, K. Miyatake, H. Uchida, M. Watanabe, J. Am. Chem. Soc. 128 (2006) 1762–1769.
[49] W. Zeng, Y. Du, Y. Xue, H.L. Frisch, in: J.E. Mark (Ed.), Physical Properties of Polymers Handbook, Springer, New York, 2007, pp. 289–303.